VALLEY CIRCULATION EXPERIMENT:

A CLASSIFICATION OF WIND FLOW IN THE

H.J. ANDREWS EXPERIMENTAL FOREST

by

Jerilyn R. Walley

A Thesis
Submitted in partial fulfillment
of the requirements for the degree
Master of Environmental Studies
The Evergreen State College
June 2013

This Thesis for the Master of Environmental Studies Degree

by

Jerilyn R. Walley

has been approved for

The Evergreen State College

by

_____
Judy Cushing
Member of the Faculty

_____
Date

ABSTRACT

Comment [JW1]: Chris wanted a longer abstract, but our styles manual limits us to 300 words.

Valley Circulation Experiment:
Using inductive analysis to classify wind flow in the
H.J. Andrews Long Term Ecological Research Forest

Jerilyn R. Walley

Week wind flow at night is a poorly understood phenomenon in the field of meteorology. The Valley Circulation Experiment (VALCEX) created a profile of wind climatology of Lookout and McRae Valleys in H. J. Andrew (HJA) using an inductive classification method. Two Sound Detection and Ranging (SoDAR) units and two sonic anemometers were installed in adjoining valleys: Lookout Valley, near HJA Headquarters meteorological station, called Primet, and McRae Valley, approximately 6 kilometers away. This instrumentation collected wind speed and direction (based on atmospheric turbulence) every 10 meters starting at 15 meters to 395 meters above ground level, aggregated to five-minute increments. Research questions for the study include: 1) Do both stations experience similar wind speeds and directions for strong and weak synoptic flow? 2) How does the moderately complex topography of HJA affect wind speed and direction? 3) Which visualizations are most suitable to display and communicate very rich time-height dependent information?

Wind flow in the two valleys showed connection during 17 non-consecutive nights of weak synoptic forcing periods with dominant flows from the north-northeast with a Valley Jet and pulsing was present (Case 1) and during 12 nights of weak synoptic forcing with flows from the north-northeast with both a Valley Jet and pulsing present (Case 2). During 13 non-consecutive nights of weak synoptic forcing with dormant flows from the southwest with No Valley Jet or pulsing (Case 3), the valleys were disconnected. The dominant factor to valley connectivity appears to be wind direction.

Keywords: Micrometeorogy, Cold-air pooling, SoDAR, Visualization

Table of Contents

Figures

Tables

Acknowledgements

It is with immense gratitude that I acknowledge all those who provided me the possibility to complete this thesis. Special appreciation goes to my reader, Dr. Judy Cushing, whose remarks and encouragement throughout this project helped me to complete my thesis, especially during the writing process.

I would like to thank Dr. Christoph Thomas, Oregon State University Biomicrometeorology Group, for introducing me to the field of Micrometeorology, and who willingly shared his precious time and equipment. Dr. Thomas conveyed a spirit of adventure in regard to this research and the daunting task of learning MATLAB.

I would like to thank my friends and family who have supported me throughout the entire process by encouraging my stick-too-it-ivness. I will be forever grateful for your love.

VALCEX was supported by Oregon State University Biomicrometeorology Group's Advanced Resolution Canopy Flow Observation (ARCFLO) campaign (NSF Career Award 0955444). Visualizing Terrestrial and Aquatic Systems (VISTAS) (NSF-DBI-1062566) supported aspects of this work.

Introduction

The Valley Circulation Experiment (VALCEX) aims to improve understanding of larger valley-scale airflow in the H.J. Andrews (HJA) Long Term Ecological Research (LTER) Forest valley. VALCEX goals include vertical structure of airflow, dynamics of cold-air drainage in the valley, and visualization techniques for interpreting results using inductive analysis. Air exchange between forests and the lower atmosphere plays an important role in transport of heat, moisture, and other trace gasses between the ground and the atmosphere, directly impacting human life and the environment (Thomas, Kennedy et al. (2011). Information relative to air exchange helps to correctly predict the spread of pollutants and contaminants for various atmospheric conditions and to more precisely estimate carbon sequestration and evapotranspiration rates from tall vegetation. How topography influences weak-wind transport is poorly understood.

A series of analyses were performed. First, the SoDAR and sonic located at headquarters were compared to a wind cup anemometer that has been collecting data for the past 20 years. Next, data from the two SoDARs were analyzed to determine connectivity within the valley under different mesoscale conditions. The second analysis was completed on 94 days of data, from March 13 through June 23. This study differs from many cold pool studies, which analyze a limited number of days (Whiteman, Zhong et al. 2001; Clements 2002; Mahrt 2008; Whiteman and Zhong 2008; Smith, Brown et al. 2009; Dorninger, Whiteman et al. 2011).

Rationale for placing the first installation near Headquarters was to compare existing meteorological instrumentation with the SoDAR and sonic, and because of existing infrastructure (power, networking capabilities). Placement of the second installation at McRae Valley was to determine connectivity within the two valleys. The McRae installation is north of the confluence of McRae and Lookout Creeks. Given that wind in the H. J. Andrews was known to flow primarily from the north-northeast, down McRae valley, or from the southwest, through Lookout and Mack Creek valleys. The hypothesis was that when wind is from the southwest, the two locations will experience different phenomena, i.e., be disconnected and when wind is from the north-northwest, the two stations will show similar speeds and directions or be connected.

1.1 The Atmospheric Boundary Layer

The Atmospheric Boundary Layer (ABL) is commonly defined as the layer of the atmosphere where the earth's surface influences wind dynamics. The sun heats the earth's surface during the day, which results in an unstably stratified ABL. This results in increasing convective driven turbulence throughout the ABL. The surface layer is the lowest portion of the ABL and is the area in which the surface fluxes are assumed to be constant with height. The largest area of the ABL is a mixed layer, just above the surface layer. The mixed layer is generally neutrally stratified. Above the ABL is an inversion layer, which separates it from the free troposphere. At night, when net radiation is negative, an inversion layer caps the mixed layer, creating a shallow Stable Boundary Layer (SBL). The SBL grows after sunset due to the surface being colder than the air above. The SBL

has generally reduced wind speeds, and wind directions can be subject to sudden shifts of up to 180°, termed "meandering" (Mahrt 2008). Weak-wind meandering has been studied less than cross-wind fluctuations yet are most directly related to practical problms, such as vertical dispersion of contaminants.

Despite the prevalence of weak-wind conditions, diurnal weak-wind transport is one of the least understood phenomena of micrometeorology (Smoot 2012). Net radiant energy is the difference between incoming and outgoing components of radiant energy. During the day, heat is transferred from the sun to the earth, called positive net radiation. During the night, the net radiant energy is negative. This shift between positive and negative net radiation leads to vertical diffusion, often creating the common phenomena of evening wind. In some situations, cold air drifts to the surface, creating pools of cold air.

1.2 Cold Air Pooling

A cold-air pool is a topographically confined, stagnant layer of air that is colder than the air above (Whiteman, Zhong et al. 2001). Whiteman et al characterized cold pools as either diurnal, forming during the evening or night and decaying following sunrise the next day, or as persistent, lasting longer than a normal night-time temperature inversion. In complex terrain, air in contact with the ground becomes cooled from radiative energy loss on a calm clear night, and being denser than the warmer air above, sinks to the valley floor (Lundquist, Pepin et al. 2008). This air can remain stagnant, trapped by the surrounding higher terrain, resulting in long periods of poor air quality and fog, depending on the

sources of pollution and amount of moisture in the air. With these very weak-wind conditions, wind direction may be quite variable (Mahrt 2008).

Cold pools begin to form in depressions, valleys, and basins in the early evening when radiant energy is negative. Cold pools can capture moisture, carbon, nitrogen and pollutants. Pools exchange energy through temperature differences, creating micro currents and turbulence. These cold-air pools, generally short term and lasting one night are called "diurnal". Cold air drainage requires large-scale wind to be weak, as strong winds will dispel the cold-air pool. According to Mahrt (2010), well-developed cold air drainage has been studied extensively from observations. Whiteman (1990) provides a detailed review of prior studies on cold pooling.

1.3 Valley Jet

A feature of airflow in complex terrain is that wind speed increases with height more rapidly than it does over level ground. Above a shallow surface shear layer, a low-level jet, or valley jet, can form as a vertical band of stronger winds in the lower part of the ABL (Arya 2001). This requires calm and widely non-turbulent conditions called stable stratification of the ALB, however some intermittent turbulence is almost always present. Under these conditions, a valley jet can occur at heights of 10 to 300 m agl (Folken 2008). Mayer defines a low level jet is a thin stream of fast moving air with maximum wind speeds of 10 ms^{-1} to 20 ms^{-1} usually located at a height of 100 to 300 m agl (2005). For this study, I have expanded this definition to include wind speed occurrences above 5 ms^{1} at heights of 100 to 250 m agl.

Instrumentation

VALCEX utilizes a paired system consisting of a Sound Detection and Ranging (SoDAR) array and a sonic anemometer for data collection, **Error! Reference source not found.**. SoDAR is a meteorological instrument used as an acoustic profiler to measure the back scattering of sound pulses for observing wind speed, wind direction, atmospheric turbulence and stability classes. SoDAR systems are used profile the lower atmosphere at heights of 15 m to more than 1,000 m agl., also called gates, of the lower atmosphere. VALCEX used a METEK mono-static phased array acoustic profiler, the PCS.2000-24.

Figure 1: SoDAR installed at Primet

The system operates by emitting an audible pulse at a defined frequency and listening for the return signal. While travelling through the atmosphere, a small fraction of the energy is backscattered and received by the antenna. The

scattering elements are small-scale air density variations due to small-scale turbulence in the air column. Analyzing the return signal intensity and the frequency, or Dopper, shift of the return signal. The return signals are analyzed by the METEK to determine wind speed, wind direction, turbulent character of the atmosphere and atmospheric reflectivity (Mayer 2005; Smoot 2012). For VALCEX, both SoDARs were programmed to take measurements every 10 m starting at 15 m and continuing to 395 m depending on atmospheric activity at a frequency of 2200 Hz. Measurements were taken every 8 seconds, then were averaged to 5 minute increments by the SoDAR. Smoot (Smoot 2012) provides comprehensive information on the use of this SoDAR system, SoDAR limitations, fixed echos and data processing.

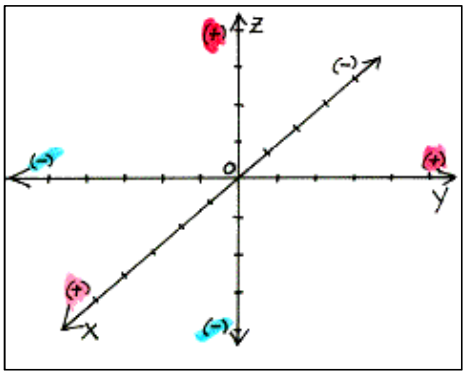

Figure 2: Cartesian coordinate system
X is oriented into the mean wind direction

Sonic anemometers use ultrasonic sound waves to measure wind speed and turbulence based on the time of flight of sonic pulses between pairs of transducers. The sonic sampled wind speed, wind direction, turbulence and temperature at a temporal resolution of 10 hz, then averaged to 5 minute increments and hourly increments. The sonic collects wind speed and direction

using three wind components, with the x-axis aligned to the direction of the mean wind, the y-axis being horizontal and the z-axis being vertical with positive upwards, **Error! Reference source not found.**

Speed and Directional Computations – Scalars v. Vectors

Wind has both a direction and a speed. The mathematical quantities used to describe wind, and all motion, fall into two categories: Scalar and Vector. Scalar quantities refer to the magnitude alone, e.g., speed, weight, time, temperature. Vector quantities refer to the both the magnitude and the direction, e.g. speed is decreasing, weight is increasing, temperature is falling, direction is northerly. SoDAR wind speed and direction data is collected using vector averages. That is, they measure the wind components, x, y, and z, as described in Figure 2, and combine the component measurements to form a wind vector at selected averaging intervals; they measure the wind components and then combine the component measurements to form a wind vector at selected averaging intervals, in this study, data was collected every 8 seconds, then averaged to 5 minute intervals.

The calculations are different between scalar and vector, for example, suppose a constant wind from 360° at 5 ms^{-1} for 5 minutes, changing to 5 ms^{-1} from 180° for 5 minutes. If averages were calculated for both vector and scalar quantities for a 10-minute period, the vector-averaged speed would be zero, whereas the scalar-averaged speed would be 5 ms^{-1}. These calculations were

performed in MATLAB using a script written by Dr. Christoph Thomas called waldschrat-aggregate_winddirection.

CHRIS – I DON'T GET THE WALSCHRAT AGG – PLEASE EXPLAIN.

Site Characteristics

HJA is situated in the north-central Oregon Cascades, near the town of Blue River, just west of the Continental Divide, Figure 3. HJA is a 15,815-acre drainage basin of Lookout and McRae Creeks, which are tributaries of Blue River and the McKenzie River. Elevation in HJA ranges from 410 to 1630 meters above sea level with roughly 1300 m elevation difference between the lowest point, near the headquarters' complex at the southwestern edge of H. J. Andrew Research Forest and the highest point at Carpenter Mountain in the northwest corner, Figure 4. McRae Creek flows southeast from its headwaters near Carpenter Mountain toward the Blue River Reservoir. Roswell Ridge raises an elevation of 1100 m between McRae and Lookout and Mack Creeks that flow from the east. They join to become Lookout Creek at 44.233147 N, -122.206421

W, just below VALCEX instrument location McRae.

Figure 3: H. J. Andrews Map, Courtesy of H.J. Andrews LTER

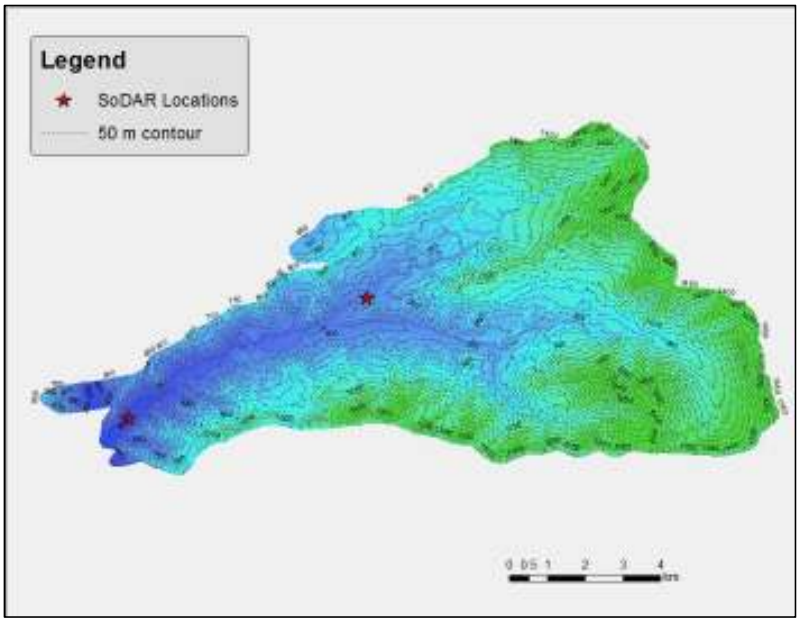

Figure 4: Topographic map of H.J. Andrews showing SoDAR locations

Instrument Placement

One SoDAR array and sonic anemometer were installed near the headquarters complex and a meteorological station that has been actively collecting data for over 20 years, referred to as Primet. It is situated at 44.211777 North, -122.255954 West, 443 meters (m) above sea level (asl). On October 14, 2011, the SoDAR was installed on a concrete pad with access to electricity and a LAN connection. The sonic anemometer was mounted on an instrumentation tower at 6.81 m above ground level (agl). As shown in Figure 5, this location is at the bottom of Lookout Creek Valley, north of the confluence of Lookout Creek and the Blue River Reservoir. North of Primet is a ridge that runs northwest at an elevation of 600 m to 800 m. To the south is a ridgeline running east-west which raises to 1,000 meters.

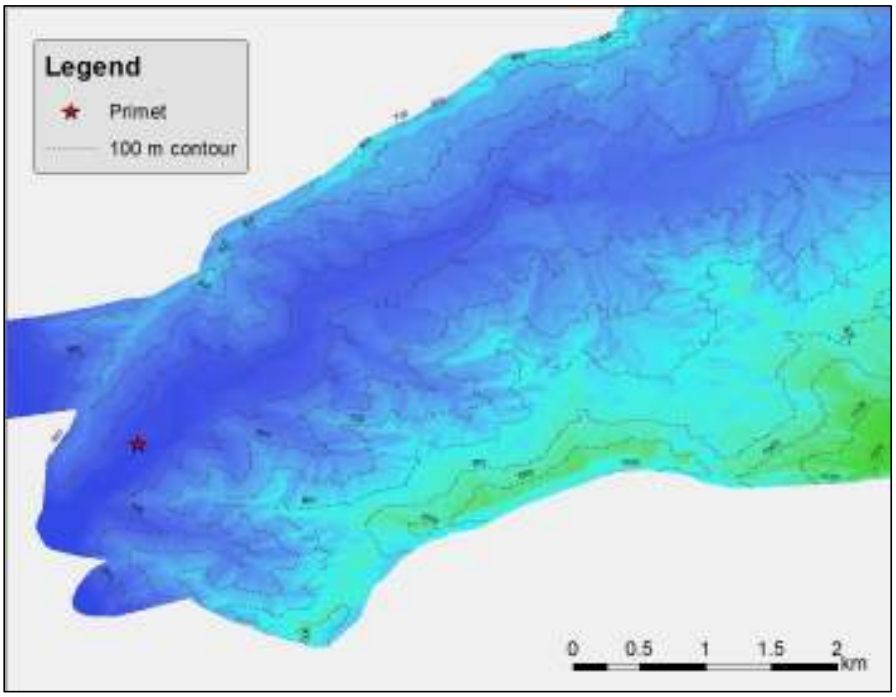

Figure 5: Primet location showing elevations

The second SoDAR array was installed October 28, 2011, up McRae Valley at Latitude 44. 24037 North, -122.19897 West, elevation 594 m asl. On November 8, the sonic anemometer was relocated to an instrument tower at 6.74 m agl. Due to lack of line power at the McRae Valley site, data collection was limited to the period between 18:00 and 8:00 Pacific Standard Time (PST). On March 12, 2012, a gasoline power generator to charge batteries was installed which enabled 24-hour data collection. The McRae location is 161 m higher in elevation than Primet. It is nestled in the McRae Creek Valley with a ridge to the south reaching elevations just over 700 m. To the north is the Blue River Ridge that reaches elevations of 1,300 m, turns west and rises to the summit of Carpenter Mountain at 1,630 m, just off the map in Figure 6. Due west of McRae is Roswell Ridge which climbs to 1,100 m before descending to Lookout Creek.

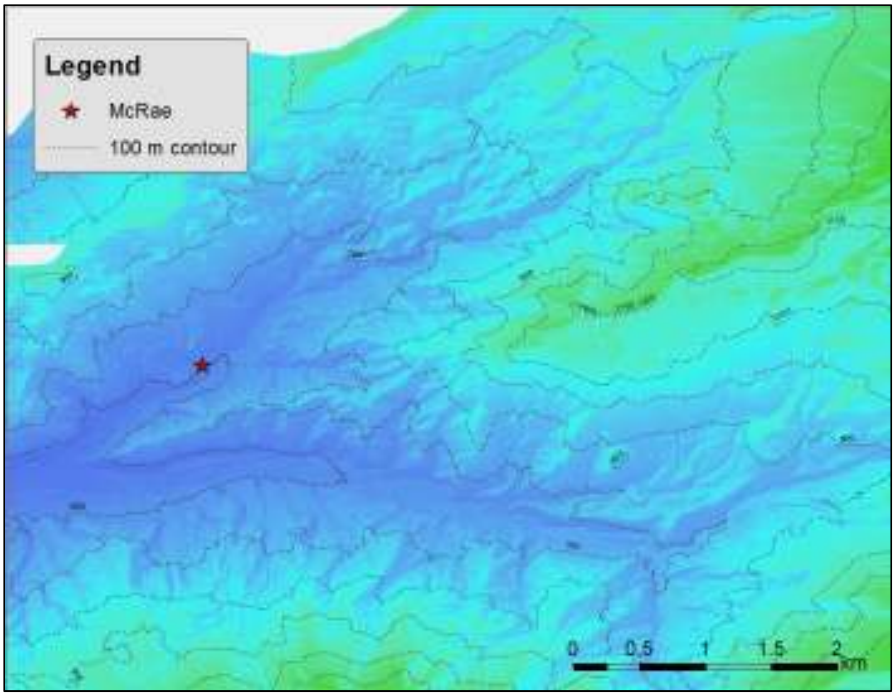

Figure 6: McRae location showing elevations

VALCEX and HJA Climate Network Station Data Comparison

Initial analysis focused on verifying the long-term meteorological network of HJA's climate network station, which includes a propeller anemometer. In contrast to the propeller anemometer, a sonic anemometer has no moving parts to measure wind speed and direction, and thus has no starting threshold. The motivation was to conduct a feasibility study extending these short-term VALCEX observations collected to the long-term historic data record measured in the HJA.

The period of November 30 to December 13, 2011, was selected for the comparison because it was dominated by weak, down-valley winds that represent one common mode of the local circulation. Both instruments were mounted at

almost the same height (sonic: ~ 8 m above ground and propeller: 10 m above ground) and in close proximity to each other. The comparison between the hourly wind speeds and directions measured with the two different instruments showed that the flows measured with the sonic anemometer were consistently stronger than those observed with the propeller anemometer (Figure 7). The averaged wind speed measured with the sonic anemometer equaled 0.35 ms-1, while that measured by the propeller anemometer was zero or significantly less than the sonic anemometer. The significant scatter in the readings of the propeller anemometer were an additional concern that arose from overspeeding of the sensor during strong gusts. Wind directions, however, agreed well with much less scatter between the two different sensors (Figure 8). We therefore conclude that the historic wind direction data collected from the propeller anemometer is meaningful and can be used to extend the wind climatology, while the wind speeds cannot be used to investigate the strength of the flows.

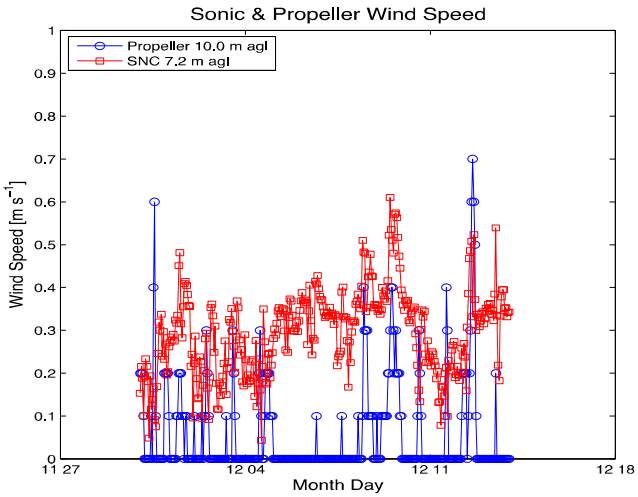

Figure 7: Distribution of wind speeds of the sonic anemometer and propeller anemometer at Primet

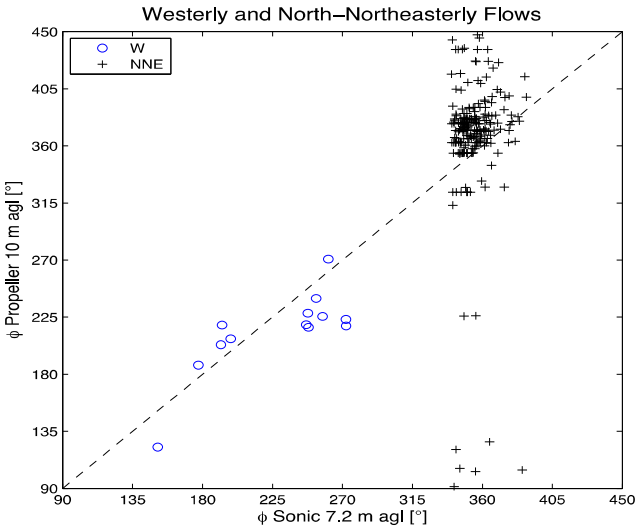

Figure 8: Comparison of wind speed between the Sonic and the cup propeller

Sodargram Analysis of 94 days

This study classified the 94 nights between March 13 and June 23, through a visual analysis of sodargrams for each 12-hour period. A sodargram is a visual

representation of aggregated data for each 5-minute period on the x-axis and each of the 41 gate heights on the Y-axis. Errors and weak signals are visualized in gray. Sodargrams are common visualizations within micrometeorology, and while these were produced in MATLAB, METEK's proprietary software includes this visualization format. For this study, wind speeds are represented on a scale from black to yellow, Figure 9. Wind direction was represented on a circular scale, with black indicating north, green representing west, blue representing south and red representing east, Figure 10.

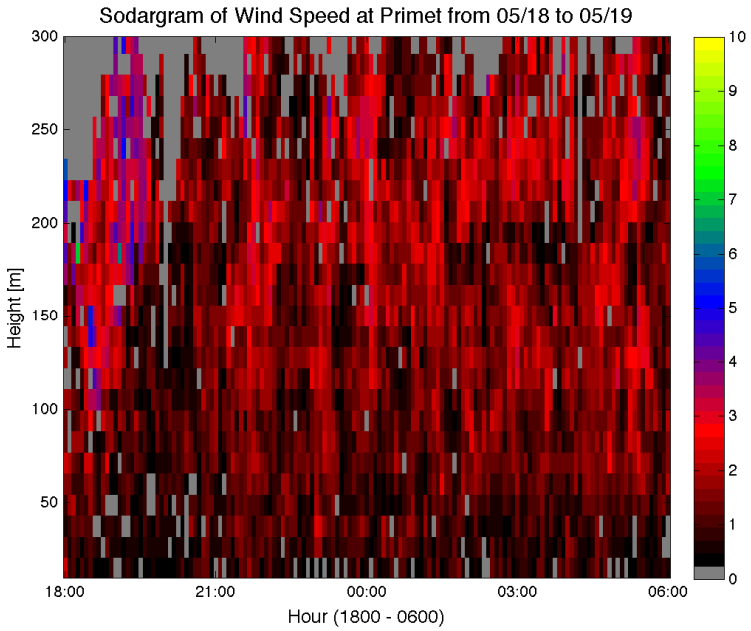

Figure 9: Speed sodargram example

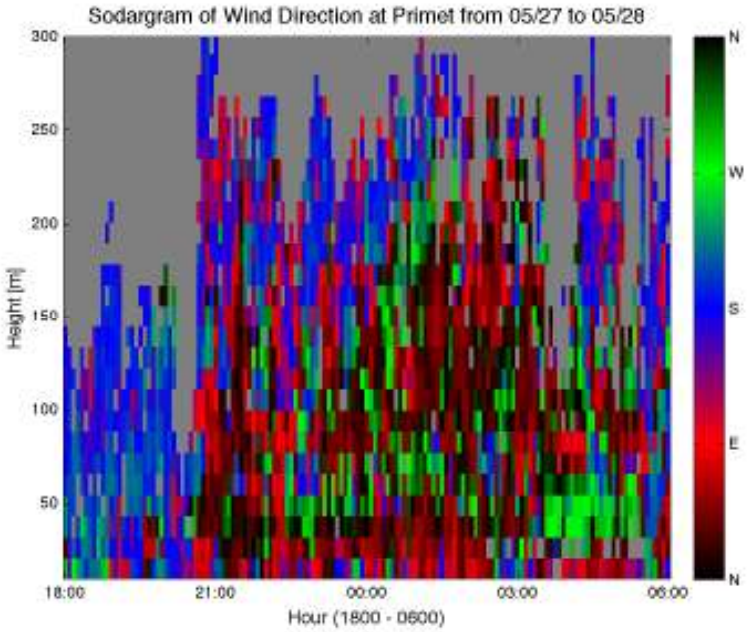

Figure 10: Directional sodargram example
Note: Color bar indicating black = N on both ends

As cold-air pooling occurs just after the sun has set, when net radiation becomes negative, the classification focused on nighttime phenomena, the period between 18:00 and 06:00. The classification used visual analysis of the data: four sodargrams for each 12-hour period were evaluated for the following phenomena:

1. Synoptic forcing (Strong or Weak)
2. Wind direction (NNE or SW)
3. Valley jet (Presence/absense)
4. Pulsing (Presence/absense)
5. Similar -henomena at both locations (Yes/No)

The each criteria was evaluated independently based on phenomena at Primet.

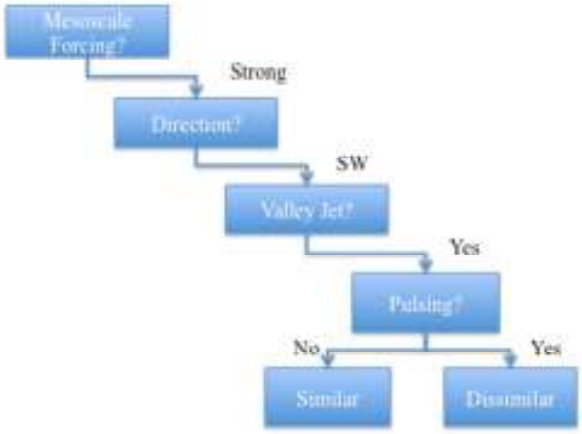

Figure 11: Diagram of decision-making process.

1.4 Classification Scheme

Each period between 18:00 p.m. and 6:00 a.m. was evaluated visually and then classified using independent five criteria using indicators shown in Table 1. The classification was based on phenomena at Primet.

Table 1: Classification Criteria

Criteria:	**Classification**		**Elevation**	**Indicator:**
Synoptic Forcing	Strong = 1	Weak = 0	50 - 300	Speeds > 5 ms^{-1}
Direction	NNE = 1	SW = 0	0 – 50	Black & Red (NNE) or Green & Blue (SW)
Valley Jet	Present = 1	Absence = 0	100 – 200	Speeds > 3 ms^{-1} btwn lower speeds above and below
Pulse	Present = 1	Absent = 0	50 - 100	Pulse of speed and direction
Similar	Similar = 1	Dissimilar = 0	NA	Yes/No

The category of Strong or Weak Synoptic Forcing was determined by presence of wind speeds above 5 ms^{-1} occurring consistently for any 6 of the 12

hour period, Figure 12. When wind speed remained below 5 ms^{-1} for the more than 6 of the 12 hour period, it was classified as Weak, Figure 13.

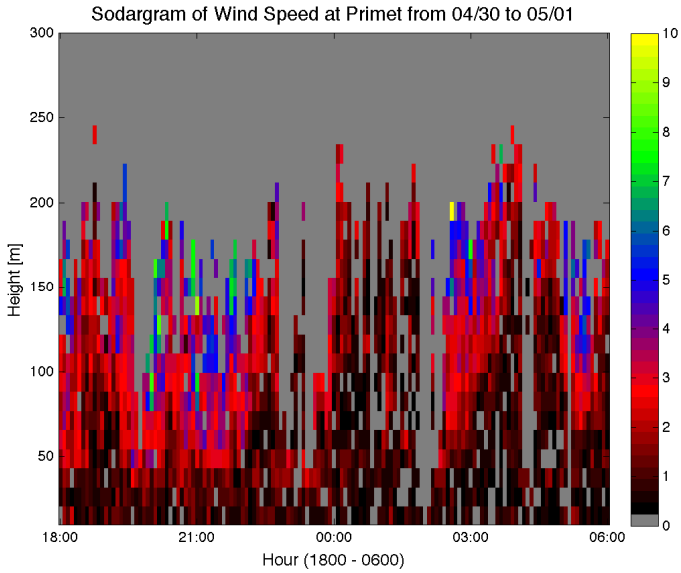

Figure 12: Strong Synoptic Forcing classification example

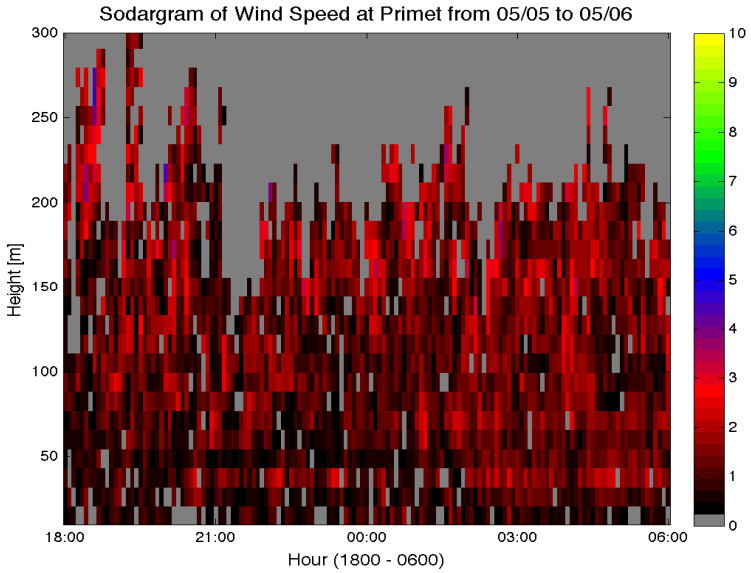

Figure 13: Weak Synoptic Forcing classification example

At low wind speeds, wind direction changes frequently and drastically, as can be seen in **Error! Reference source not found.** on page 12. To determine directional classification for a 12-hour period, gate heights between 0 and 50 m agl were evaluated to determine the primary flow direction.

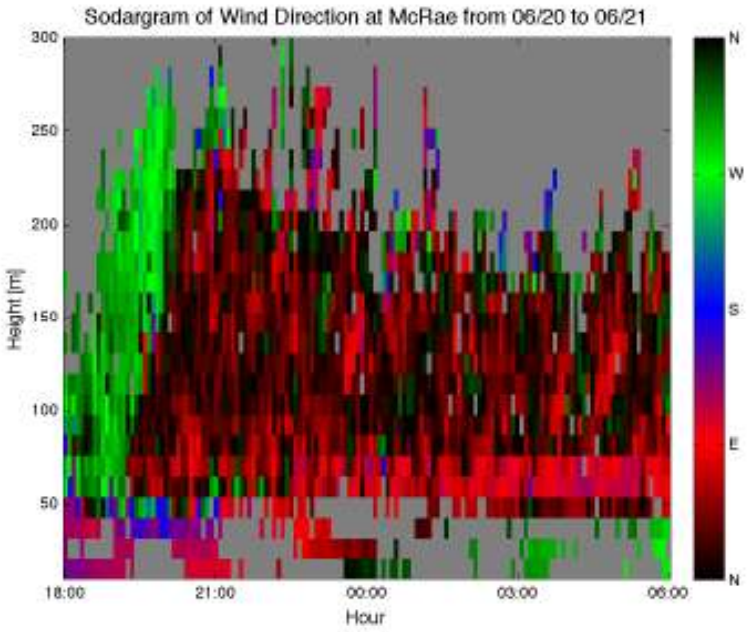

Figure 14: NNE wind direction classification

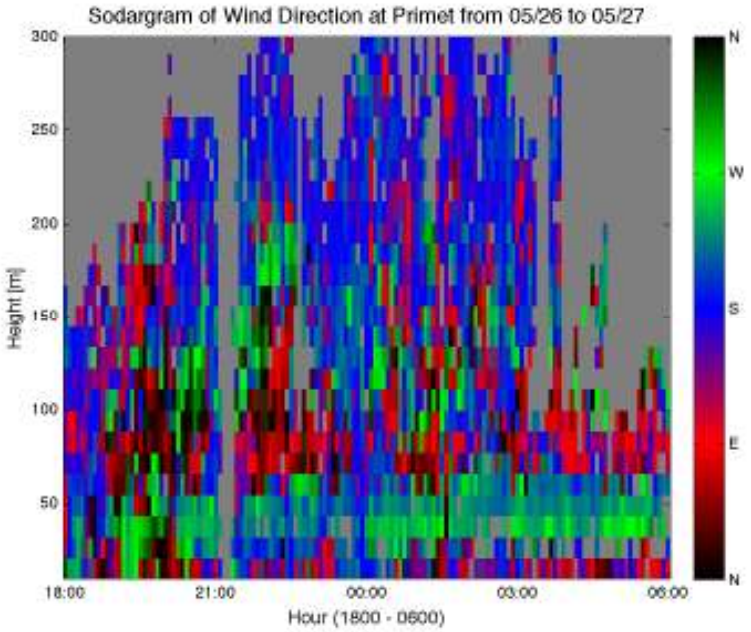

Figure 15: SW wind direction classification

The third classification criterion is the presence or absence of a Valley Jet, a band of higher wind speed at approximately 100 – 200 m agl. This phenomenon does not fit the classic definition of low-level jet as the speeds are not above 10 ms^{-1}. The Valley Jet can be seen as a band of higher speeds, between 2.5 and 4 ms^{-1}, nested between lighter wind, as shown in the circled area on Figure 16. The Valley Jet was present more in McRae Valley; if the Valley Jet was present in that location, the entire night was classified as "VJ Present".

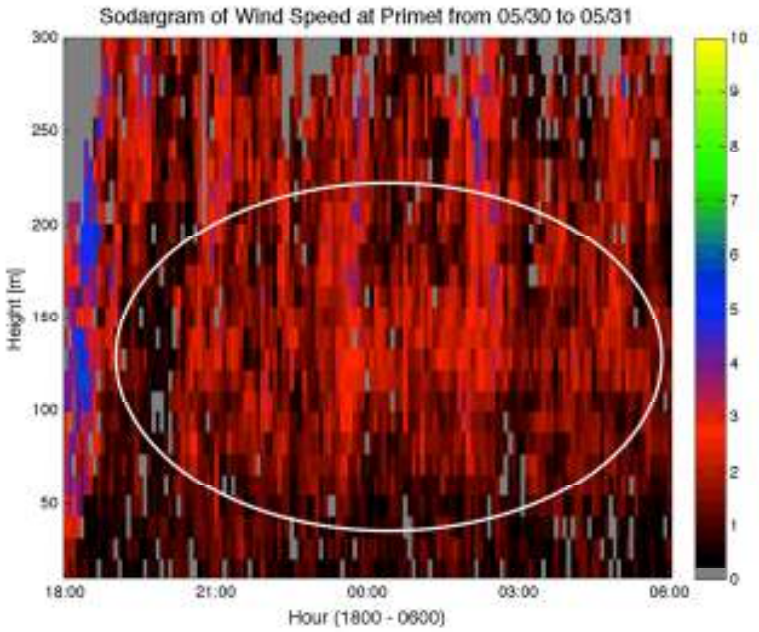

Figure 16: Valley jet classification example (in circle)

The fourth phenomenon evaluated was the presence or absence of pulsing or alternating wind directions at between 50 and 100 m agl, called pulses. The pulse starts at lower elevations, around 40 m agl, then raises to approximately 100 m agl, so it can be seen as a pattern of directional shifts, Figure 17 and Figure 18.

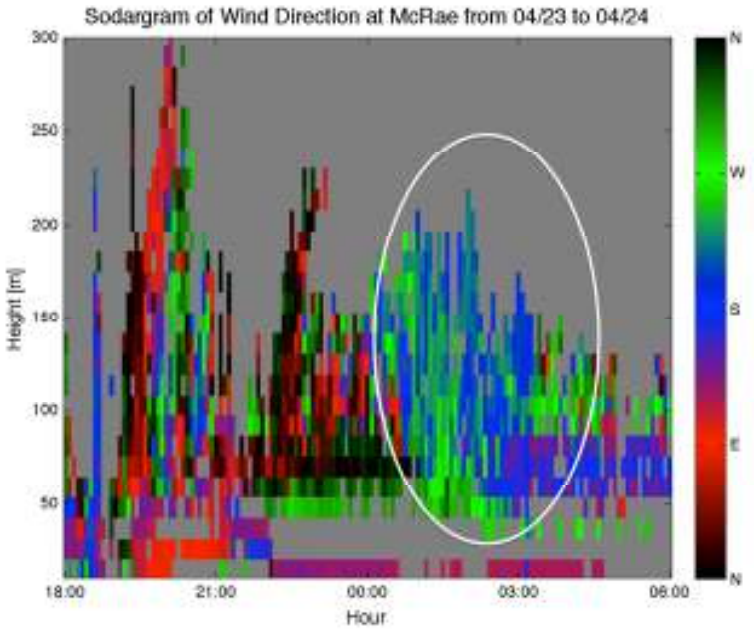

Figure 17: Pulse wind direction classification example (in circle)

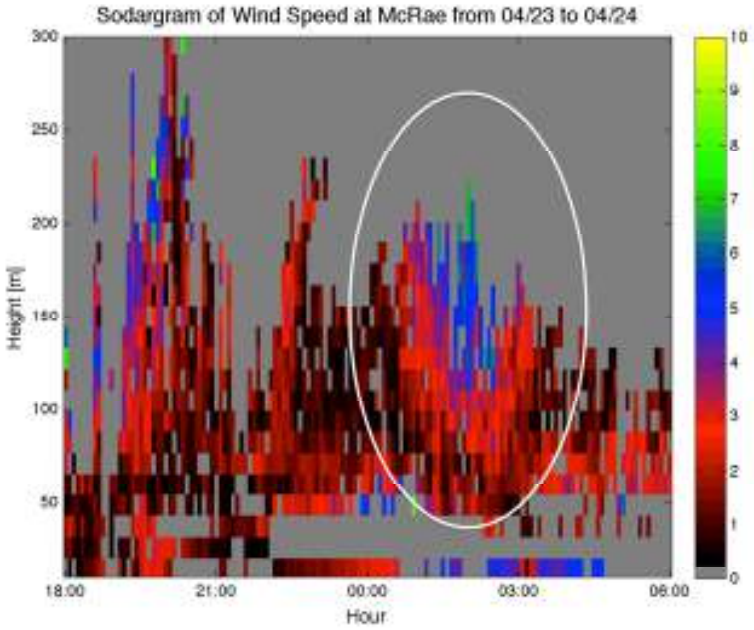

Figure 18: Pulse wind speed classification example (in circle)

The final classification criterion was Similar or Dissimilar. This criterion indicates whether the two locations are similar or dissimilar for wind speeds and directions. This criterion evaluates the connectivity within the valley.

Cases based on classification criteria

Based on the five-category classification, 36 cases were possible. The three most common cases were:

- Case 1: Weak SF, NNE flows, Valley Jet, No Pulse, Similar (17 nights);
- Case 2: Weak SF, SW flows, No Valley Jet, Pulse Dissimilar (13 nights)
- Case 3: Weak SF, NNE, Valley Jet, Pulse, Similar (12 nights).

The 13 cases with 0 to 3 nights meeting the criteria were not analyzed.

Table 2: Number of Nights by Case shows the 32 possible cases and the number of days meeting each criterion. The analysis focuses on cases with 4 or more nights meeting the criteria.

Table 2: Number of Nights by Case

Case	Synoptic Forcing	Flow Direction	Valley Jet	Pulse	Similar	Number of Nights	Page Number
1	Weak	NNE	Yes	No	Yes	17	**Error! Bookmark not defined.**
2	Weak	SW	No	Yes	No	13	31
3	Weak	NNE	Yes	Yes	Yes	12	33
4	Weak	NNE	No	Yes	No	9	35
5	Weak	SW	No	Yes	Yes	6	36
6	Strong	SW	No	Yes	No	6	37
7	Weak	SW	No	No	No	5	39
8	Weak	SW	Yes	Yes	Yes	5	38
9	Weak	NNE	Yes	Yes	No	5	40
10	Weak	SW	Yes	No	No	4	41

11	Weak	NNE	No	No	No	4	42
12	Weak	NNE	Yes	No	No	3	
13	Strong	NNE	Yes	No	Yes	3	
14	Strong	NNE	No	Yes	Yes	2	
15	Strong	SW	No	No	No	1	
16	Strong	SW	No	No	Yes	1	
17	Strong	SW	No	Yes	Yes	1	
18	Strong	SW	Yes	No	No	1	
19	Strong	SW	Yes	No	Yes	1	
20	Strong	NNE	No	No	No	1	
21	Strong	NNE	No	Yes	No	1	
22	Weak	SW	No	No	Yes	0	
23	Weak	SW	Yes	No	Yes	0	
24	Weak	SW	Yes	Yes	No	0	
25	Weak	NNE	No	No	Yes	0	
26	Weak	NNE	No	Yes	Yes	0	
27	Strong	SW	Yes	Yes	No	0	
28	Strong	SW	No	Yes	Yes	0	
29	Strong	NNE	No	No	Yes	0	
30	Strong	NNE	Yes	No	No	0	
31	Strong	NNE	Yes	Yes	No	0	
32	Strong	NNE	Yes	Yes	Yes	0	

1.5 Mean wind climatology over entire period: March 13 through June 13

Five-minute speed and direction data were averaged by gate height for 94 nights between 1800 and 0600 (Figure 19). Wind speeds in the McRae Valley are generally very weak, below 1 ms^{-1} at elevations below 195 m agl. Above 205 m agl speeds increase with speeds being generally greater at the McRae station than at Primet. The error bars for each gate show increasing variation with elevation. Directional averages show a disconnect between Primet and McRae, with averages at Primet being south at lower elevations and changing to east between 100 and 200 m agl and north-northeast above 200 m agl. At McRae, on the other hand, flows above 50 m agl and below 100 m agl vary between south and west,

Comment [JW2]: Chris had a note here I can't read.

moving to from the west between 100 and 300 m agl; above 300 m agl, flows again vary between south, southeast and north. Near zero wind speed variation, shown by error bars, is the result of opposing flows with similar magnitude, so the resultant vector speed is near zero.

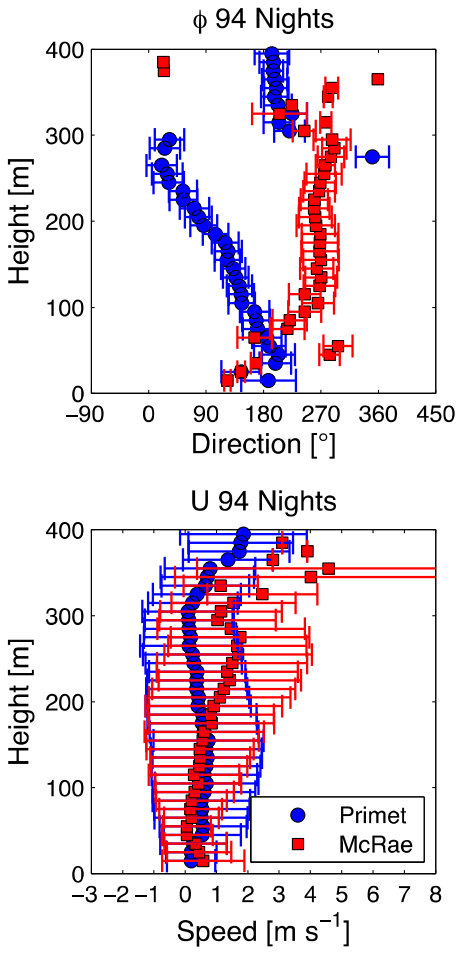

Figure 19: Speed and direction averages by height for all 94 nights

1.6 Case 1 – Weak SF NNE Valley Jet No Pulse Similar

Seventeen nights met the classification criteria for Weak SF, NNE flow, Valley Jet, Pulse, Similar. The 17 days were ensemble-averaged (Figure 20). The two SoDARs (Primet and McRae Valley) show similar wind speeds at all elevations between 0 and 2 ms^{-1}. Standard deviation increases with elevation; McRae has greater variability between 200 and 300 m agl. Flows for both stations averaged between 0° and 45° at gates below 200 m agl. Above 200 m, directions shift to between 300° and 260°. The Valley Jet is weak, speeds approximately 0.5 m faster at between 100 and 160 m agl and can be seen by increased speeds creating a slight 'nose'. This case shows connectivity between the two stations.

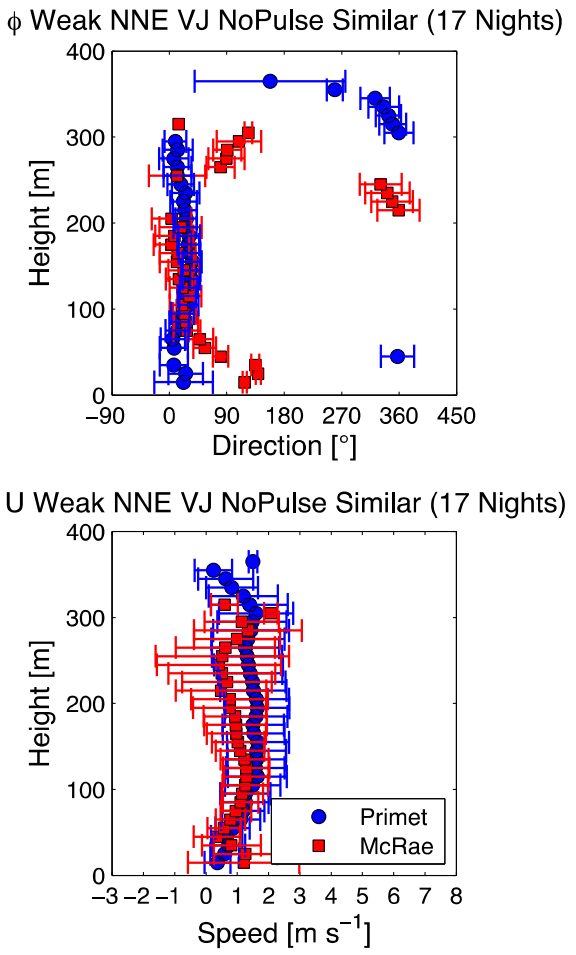

Figure 20: Speed and direction averages by height for Case 1

1.7 Case 2 – Weak SF SW No Valley Jet Pulse Dissimilar

Thirteen nights met the classification criteria for Weak SF, SW flow, No Valley Jet, Pulse Dissimilar. These 13 days were ensemble-averaged (Figure 21). The two SoDARs show dissimilar wind speeds at elevations above 130 m agl, with speeds between above 1 ms^{-1} and speeds increasing at McRae while remaining below 2 ms^{-1} at Primet. Wind speeds increase in variability as elevation increases, with McRae having larger standard deviation at all elevations. Directions for these averaged nights are different, with McRae directions varying at the lower elevations, turning to northwest above. Primet is varied at all elevations, but tending towards 270° at higher elevations. In this case, flows the McRae Valley are disconnected those in the larger Lookout Creek Valley.

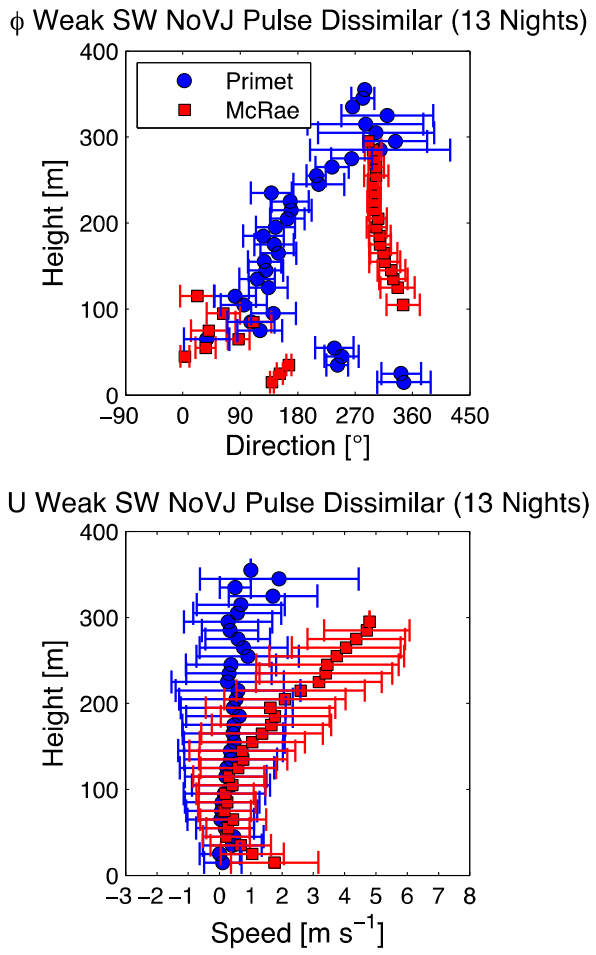

Figure 21: Speed and direction averages by height for Case 2

Case 3 – Weak SF NNE Valley Jet Pulse Similar

Twelve nights met the classification criteria for Strong SF, NNE flow, Valley Jet, Pulse, Similar, and were also ensemble-averaged (Figure 22). The two SoDARs show a strong positive correlation in this case. Primet and McRae show wind speeds at elevations below 300 m agl are weak, below 1.5 ms^{-1} at all gate heights. Wind direction for McRae and Primet averaged between 0 and 45° below 300 m agl, shifting to north at gates above 300 m agl. McRae directions change from southerly to northerly and back to southerly as elevation increases. Variability of wind direction is small in this case. There does appear to be a connection between McRae and Lookout Creek in Case 3.

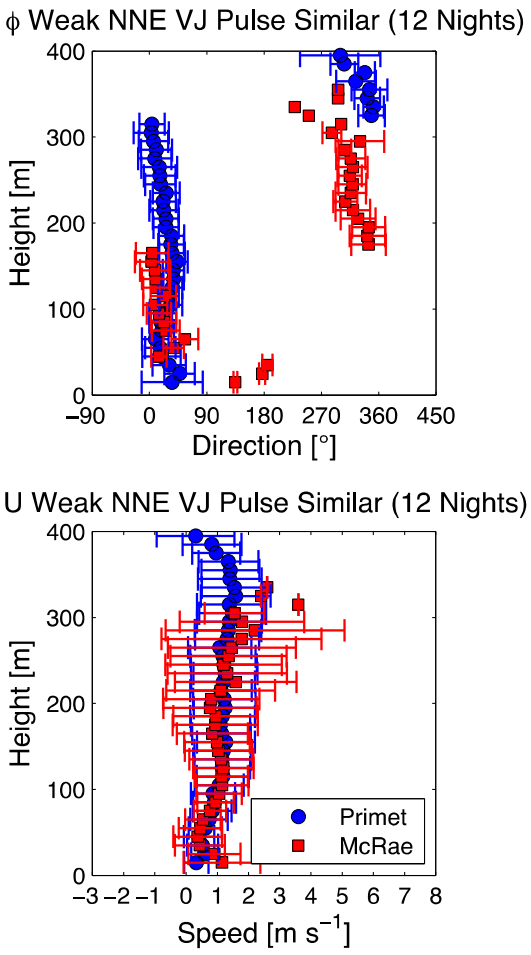

Figure 22: Speed and direction averages by height for Case 3

1.8 Case 4 – Weak SF NNE No Valley Jet Pulse Dissimilar (9 nights)

Nine nights met the classification criteria for Weak SF, NNE flows, No Valley Jet, Pulse, Dissimilar (Figure 23). While wind speeds were similar, wind directions for this case were different between the two stations, with McRae varying extensively at all gate heights. Speeds for both stations range below 1 ms^{-1} below 200 m agl. Above 200 m agl, speeds increase to 3 ms^{-1}.

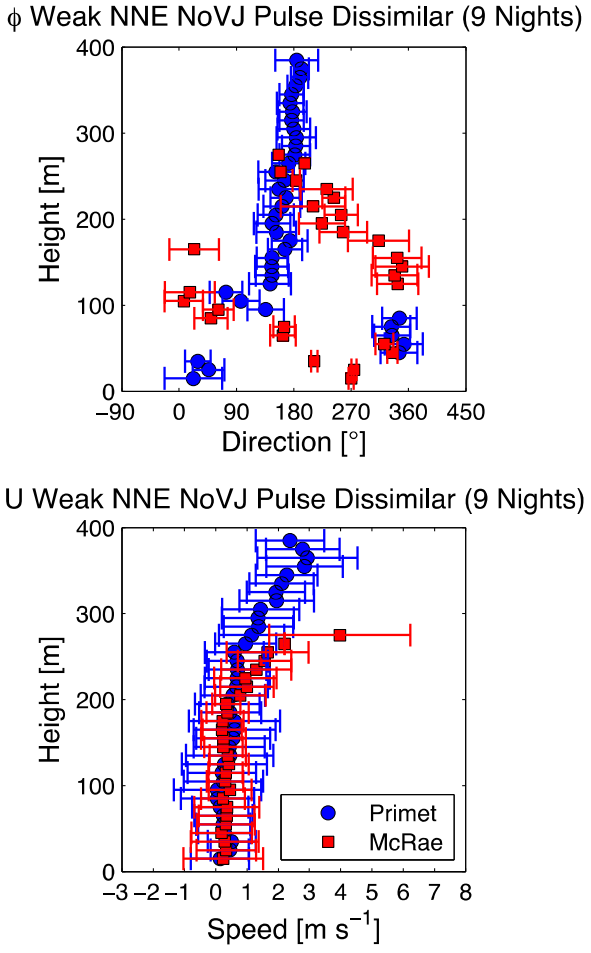

Figure 23: Speed and direction averages by height for Case 4

1.9 Case 5 – Weak SF, SW, No Valley Jet, Pulse, Similar (6 Nights)

Six nights met the classification Weak SF, SW, No Valley Jet, Pulse, Similar (Figure 24). Speeds for the two locations were relatively similar, however a weak valley jet was seen at McRae and not at Primet. The directions are approximately 90° different between the two locations, but were similar at lower elevations.

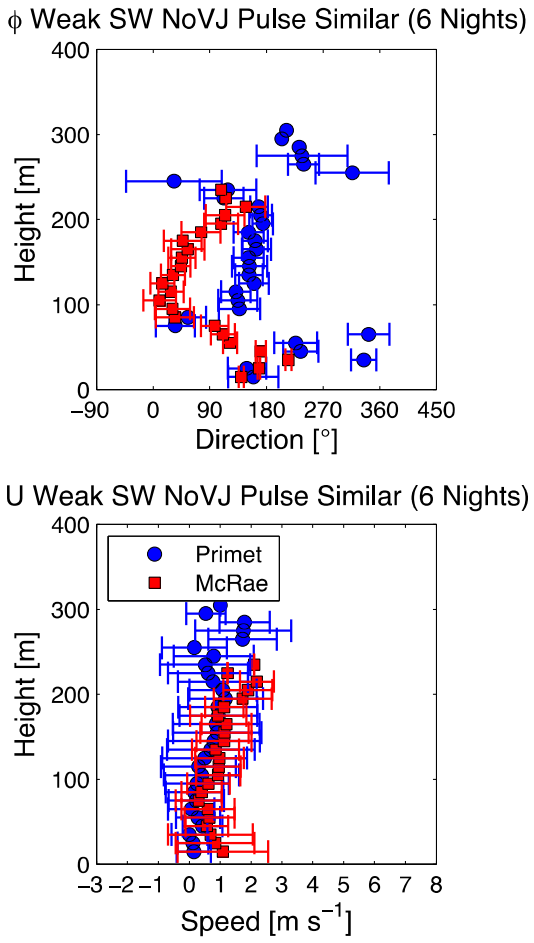

Figure 24: Speed and direction averages by height for Case 5

1.10 Case 6 – Strong SF, SW, No Valley Jet, Pulse, Dissimilar (6 Nights)

Six nights met the classification Strong SF, SW, No Valley Jet, Pulse, Dissimilar (Figure 25). The directions were between 45° and 90° different between the two locations, but were similar at lower elevations. Primet directions average due south while McRae varies from north to west and back again as elevation increases. Wind speed for the McRae averages below 1 ms^{-1} at lower gate heights with the exception of the first at 15 m agl, then increase above 240 m agl to above 1 ms^{-1}. Primet's wind speeds increase consistently with gate height.

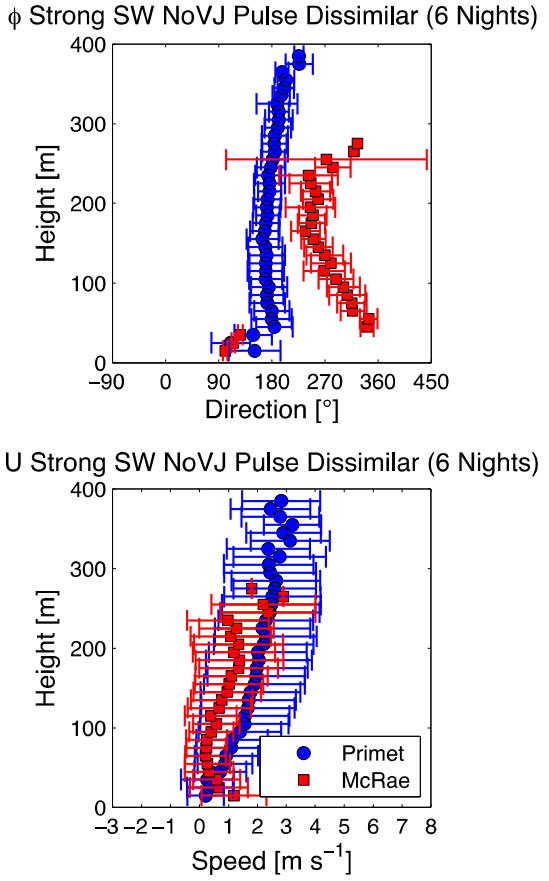

Figure 25: Speed and direction averages by height for Case 6

1.11 Case 7 – Weak SF, SW, Valley Jet, Pulse, Similar (5 Nights)

Five nights met the classification Weak SF, SW, Valley Jet, Pulse, Similar (Figure 26) Speeds for the two locations were relatively similar, with a valley jet showing at both locations. The directions were approximately 90° different below 50 meters, but were very similar above.

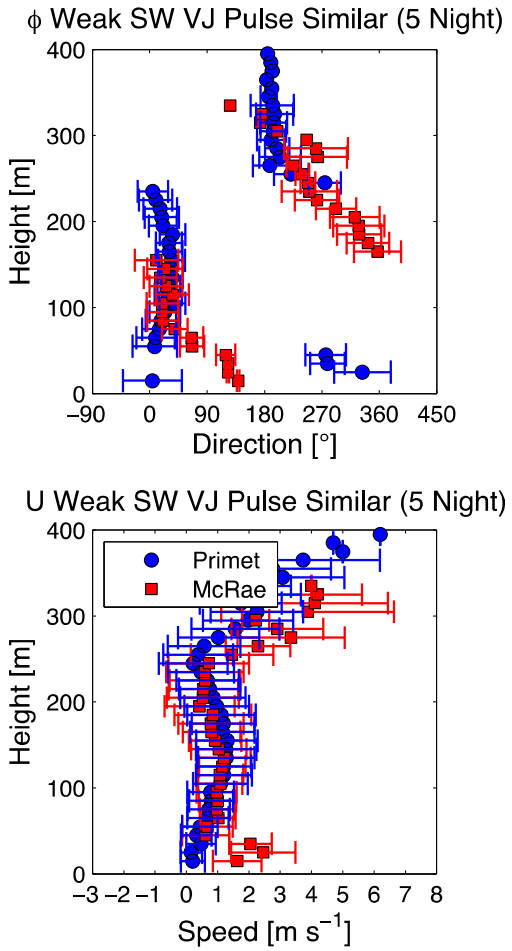

Figure 26: Speed and direction averages by height for Case 7

1.12 Case 8 – Weak SF, SW, No Valley Jet, No Pulse, Dissimilar (5 Nights)

Five nights met the classification Weak SF, SW, No Valley Jet, Pulse, Disimilar (Figure 27). Primet was consistent for both speed and directions at all elevations, while McRae speeds increase steadily above 200 meters and directions vary at lower elevations, becoming southerly at above 100 m agl.

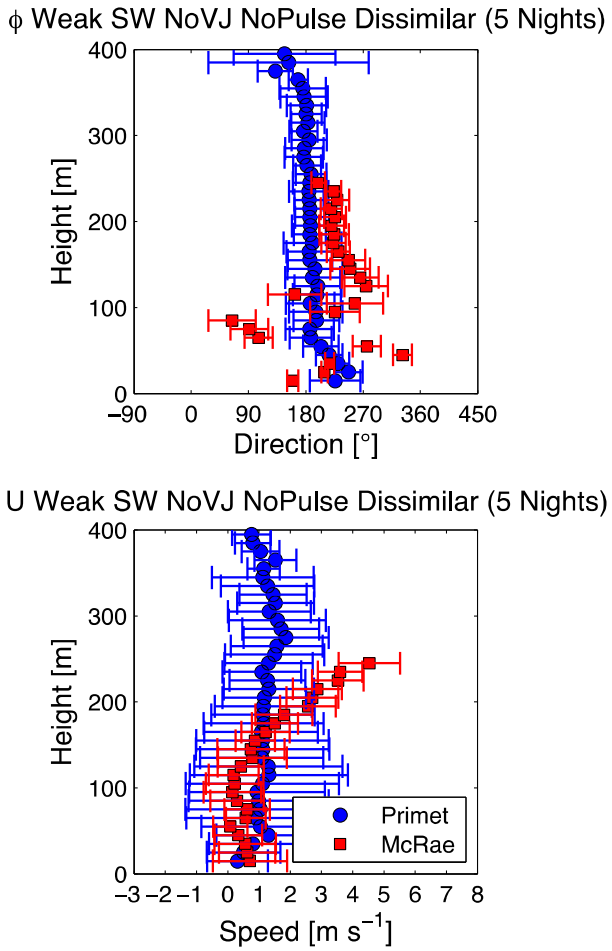

Figure 27: Speed and direction averages by height for Case 8

1.13 Case 9 – Weak SF, NNE, Valley Jet, Pulse, Dissimilar (5 Nights)

Five nights met the classification Weak SF, SW, Valley Jet, Pulse, Disimilar (Figure 28). Speeds for both locations were extremely similar, showing a Valley Jet at approximately 150 m and slowing at approximately 250 m before picking up again above. Direction varies at low elevation and becomes extremely similar above 50 m. The averages for this case show such similarities that it's surprising these were classified as dissimilar when evaluating the sodargrams.

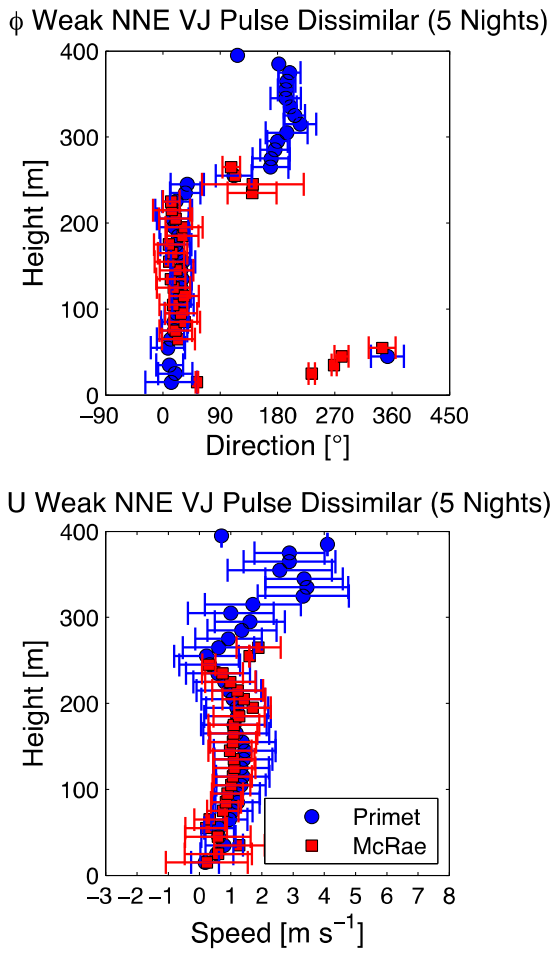

Figure 28: Speed and direction averages by height for Case 9

1.14 Case 10 – Weak SF, SW, Valley Jet, No Pulse, Dissimilar (4 Nights)

Four nights met the classification Weak SF, SW, Valley Jet, No Pulse, Dissimilar (Figure 29). Speeds for both locations were below 1 ms^{-1}, with McRae showing a valley jet at between 150 and 200 m agl, which Primet does not experience. Direction varies at low elevation at Primet while McRae is consistently below 1 ms^{-1} until about 250 m.

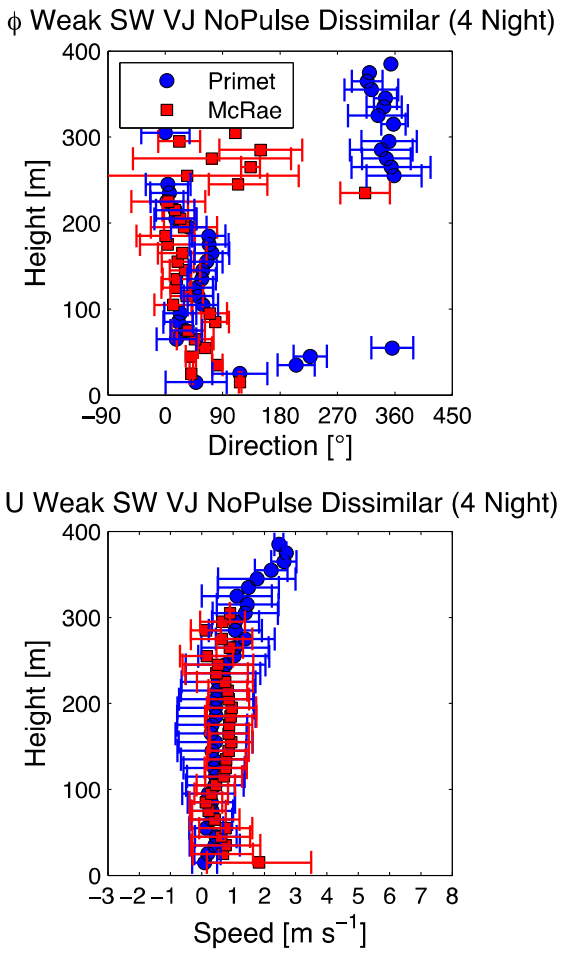

Figure 29: Speed and direction averages by height for Case 10

1.15 Case 11 – Weak SF, NNE, No Valley Jet, No Pulse, Dissimilar (4 Nights)

Four nights met the classification Weak SF, NNE, No Valley Jet, No Pulse, Dissimilar (Figure 30). This case shows variation in both wind speed and direction at all elevations.

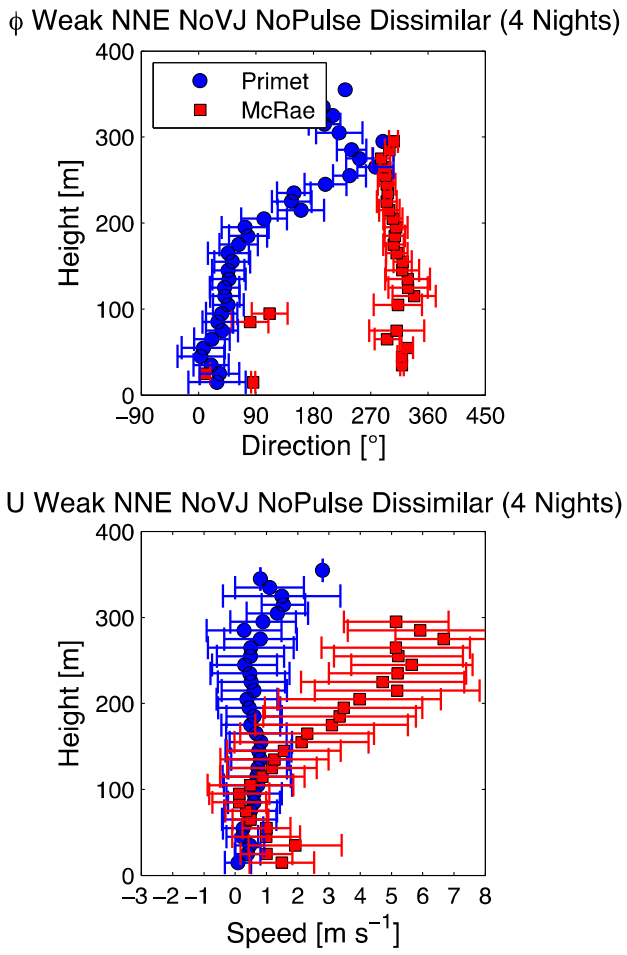

Figure 30: Speed and direction averages by height for Case 11

Summary

Of the 94 days, weak synoptic forcing dominated, with 79 nights classified in this criterion. The remaining criteria were almost equally distributed: North northeast had 52 nights while SW flows were found on 42 nights; the Valley Jet was present on 49 nights; pulsing was present 56 nights, and the phenomena were

similar on 49 nights (Table 3). These valleys are dominated by weak winds, either from the north-northeast or the southwest.

Table 3: Number of nights meeting each criterion

Criterion	Classification	# Nights	Classification	# Nights
Synoptic Flow	Weak	79	Strong	15
Wind Direction	SW	42	NNE	52
Valley Jet	Absent	45	Present	49
Pulsing	Absent	38	Present	56
Similar	Similar	49	Dissimilar	45

Wind direction flows under two dominant regimes, from the north-northeast or from the southwest. On 52 nights the wind flow was downvalley from the north-northeast. The wind direction was up-valley from the southwest, the remaining 42 nights. When combined with Synoptic Forcing, the study period had 38 nights of Strong SF with flow from the SW, 14 nights of Strong SF and flows from the NNE, 11 nights of Weak SF with flows from the SW, and 31 nights of Weak SF with flows from the NNE. During the study period, the valley jet was present 49 of the 94 nights. Pulses were present 56 nights, generally when the dominant direction was from the north-northeast. There were 45 nights with similar phenomena at the stations.

In the 11 cases evaluated, weak synoptic forcing dominated with only one case showing strong synoptic forcing (Table 4). This demonstrates that the area generally has wind speeds below 2 ms^{-1}, so speed is not a good indicator of connectivity. Connectivity between Lookout and McRae Valleys is most closely related to dominant wind direction, with connection occurring generally when winds were from the north-northeast. The large variation in direction is due in

part to the weak wind regime and to classifying based on the lowest 50 m agl. There seems to be a connection between connectivity of the valleys and the presence of the Valley Jet, which occurred in every case of valley connectivity and appeared in only one case of disconnection.

Table 4: Connectivity by Case

Case Number	Synoptic Forcing	Flow Direction	Valley Jet	Pulse	Similar	Number of Nights	Valleys Connected
1	Weak	NNE	Yes	No	Yes	17	Yes
2	Weak	SW	No	Yes	No	13	No
3	Weak	NNE	Yes	Yes	Yes	12	Yes
4	Weak	NNE	No	Yes	No	9	No
5	Weak	SW	No	Yes	Yes	6	No
6	Strong	SW	No	Yes	No	6	No
7	Weak	SW	No	No	No	5	No
8	Weak	SW	Yes	Yes	Yes	5	Yes
9	Weak	NNE	Yes	Yes	No	5	Yes
10	Weak	SW	Yes	No	Yes	4	Yes
11	Weak	NNE	No	No	No	4	No

Comment [JW3]: Judy, I think this is where Chris' suggestion of combining cases should go.

Discussion

It is interesting to note that 3 of the 5 cases were not classified as similar even though the valleys appear connected. However, to conclusively determine if this analysis was effective, an algorithmic analysis could be completed as a comparison.

Future Work & Recommendations

Given unlimited time and resources I would make a few changes to this project. First, I would have limited my classification criteria to two or three phenomena; synoptic forcing, dominant wind direction, with possible inclusion of the valley jet. Limiting the number of phenomena evaluated would allow for fewer cases, which would create a stronger correlation between phenomena and valley connectivity.

Wind direction variability is the nature of weak wind. In regards to classifying flow direction, is limited by categorizing into two dominant directions. Looking back, I would have created four directional categories; NW, NE, SW, and SE. This would allow for classifying sodargrams with wind directions not easily lumped into NNE or SW.

Second, I would use multiple visualization techniques, comparing sodargrams to windroses, or another visualization. A study of that type could be extremely interesting in determining which methods of visualization most effectively display and communicate this data-rich information. It would be extremely helpful and telling to input this data into VISTAS software for further visual analysis. To take this change one step further, it would be interesting to review visualizations used in other disciplines, namely hydrology, to see if they could be used to visualize micrometeorological phenomena. Hydrology and meteorology are both the study of fluids in motion. Previous work for the VISTAS project resulted in reviewing hundreds of visualizations from four hydrology journals. During this review, I noticed that hydrologists have interesting visualizations and modeling software programs.

This project was extremely data intensive, requiring a specialized use of MATLAB, a programming language for science and engineering. I found this part of the project extremely difficult. It is my recommendation that future researchers have a prior experience in both programming and physics.

Bibliography

Arya, P. S. (2001). Introduction to micrometeorology. London, Academic Press.

Clements, C. (2002). "Cold-Air-Pool Structure and Evolution in a Moutain Basin: Peter Sinks, Utah." Journal of Applied Meteorology and Climatology **42**.

Dorninger, M., C. D. Whiteman, et al. (2011). "Meteorological Events Affecting Cold-Air Pools in a Small Basin." Journal of Applied Meteorology and Climatology **50**(11): 2223-2234.

Folken, T. (2008). Micrometeorology. Verlag Berlin Heidelberg, Springer.

Lundquist, J. D., N. Pepin, et al. (2008). "Automated algorithm for mapping regions of cold-air pooling in complex terrain." Journal of Geophysical Research **113**(D22).

Mahrt, L. (2008). "Mesoscale wind direction shifts in the stable boundary layer." Tellus Series A-Dynamic Meteorology and Oceanography **60A**: 700-705.

Mahrt, L., S. Richardson, et al. (2010). "Non-stationary drainage flows and motions in the cold pool." Tellus A: no-no.

Mayer, J.-C. (2005). Characterization of the atmospheric boundary layer in a complex terrain using SODAR-RASS. Master of Science in Geoecology, University of Bayreuth.

Smith, S. A., A. R. Brown, et al. (2009). "Observations and Simulations of Cold Air Pooling in Valleys." Boundary-Layer Meteorology **134**(1): 85-108.

Smoot, A. R. (2012). Linking dynamics of the near-surface flow to deeper boundary layer forcing in the nocturnal boundary layer. Masters of Science, Oregon State University.

Thomas, C. K., A. M. Kennedy, et al. (2011). "High-Resolution Fibre-Optic Temperature Sensing: A New Tool to Study the Two-Dimensional Structure of Atmospheric Surface-Layer Flow." Boundary-Layer Meteorology **142**(2): 177-192.

Whiteman, C. D. (1990). "Observations of thermally developed wind systems in mountainous terrain." Atmospheric processes over complex terrain, Meteor. Monogr **23**(45): 5-42.

Whiteman, C. D. and S. Zhong (2008). "Downslope Flows on a Low-Angle Slope and Their Interactions with Valley Inversions. Part I: Observations." Journal of Applied Meteorology and Climatology **47**(7): 2023-2038.

Whiteman, C. D., S. Zhong, et al. (2001). "Cold Pools in the Columbia Basin." Weather and Forcasting **16**.